Transportation Research Part D 88 (2020) 102528

Contents lists available at ScienceDirect

Transportation Research Part D

journal homepage: www.elsevier.com/locate/trd

Fuel Estimation in Air Transportation: Modeling global fuel consumption for commercial aviation

K. Seymour*,[1], M. Held*,[1], G. Georges, K. Boulouchos

ETH Zürich (Swiss Federal Institute of Technology Zurich), Institute of Energy Technology, Laboratory of Aerothermochemistry and Combustion Systems, Energy Systems Group, Sonneggstrasse 3, 8092 Zurich, Switzerland

ARTICLE INFO

Keywords:
Aircraft fuel burn model
Commercial aviation CO_2 emissions
Global flight movements
Global aircraft fuel consumption
EUROCONTROL BADA
Carbon dioxide emissions inventory

ABSTRACT

Accurate fuel burn estimation models are required to assess potential reductions in CO_2 emissions stemming from new aircraft technologies.

This study provides a novel framework for *Fuel Estimation in Air Transportation (FEAT)*: a two-component approach comprising of (1) a high fidelity flight profile simulator based on the aircraft performance model from EUROCONTROL, and (2) a reduced order fuel consumption approximation with origin-destination airport pair and aircraft type as sole inputs. The latter allows for accurately estimating fuel consumption for global scheduled aircraft movements of an entire year in a matter of milliseconds. We calculate total CO_2 emissions from scheduled commercial aviation in 2018 to be 812 Mt. The modeling error of fuel consumption is validated against fuel burn reports and ranges below 5%.

Current aircraft performance models either focus on fuel estimation accuracy or on computational efficiency. Combining both, *FEAT* enables rapid assessment of decarbonization strategies for commercial passenger aviation.

1. Introduction

In an increasingly connected world, the climate impact of commercial aviation is expected to grow rapidly. Continued airline fuel efficiency gains of 2% per annum on average in the period since 2009 have partially decoupled CO_2 emissions from increasing air traffic, but the average 3% per annum increase in estimated CO_2 emissions during the same period demonstrates the overwhelming influence of traffic growth in aviation (ATAG, 2020). In 2019 an estimated 8.68 trillion revenue passenger-kilometers (RPK) were performed by the worldwide airline industry (IATA, 2019). This is a 4.2% increase over the 8.33 trillion performed in 2018 (IATA, 2019) and falls largely in line with predicted compound annual growth rates over the period from 2015 to 2035 from Boeing, Airbus, Embraer, and the International Civil Aviation Organization (ICAO, 2019).

For evaluating the current and future climate impact of commercial aviation, robust aircraft fuel consumption and emissions models are indispensable. In the most basic form of bottom-up fuel consumption modeling, complete flights are approximated by a single cruise phase in some form of the Breguet range equation (Lee et al., 2001). However, this poorly captures other critical flight phases, commonly divided into taxi, take-off, climb, descent, approach, and landing. On the other hand, physics-based 4D aircraft trajectory simulations are often utilized to accurately predict fuel consumption and localized emissions (Ahearn et al., 2017). Generally, utilization of complex models is limited by high computational cost and alleviation of complexity comes at the expense of

* Corresponding authors.
E-mail addresses: seymourk@ethz.ch (K. Seymour), held@lav.mavt.ethz.ch (M. Held).
[1] These authors equally contributed to this work.

https://doi.org/10.1016/j.trd.2020.102528

Available online 09 October 2020

non-public data. Yanto and Liem (2018) provide a review of various fuel burn models varying in computational complexity and modeling accuracy. Other reviews include models used for emissions inventories (Olsen et al., 2013; Skowron et al., 2013; Wasiuk et al., 2015).

One such emissions inventory tool is the United States Federal Aviation Administration's (FAA) Aviation Environmental Design Tool (AEDT), which enables high temporal and spatial resolution predictions of fuel burn and emissions from commercial aviation. It was developed to provide a method for evaluating effects of policy, technology, and operational scenarios on aircraft fuel use and emissions (Ahearn et al., 2017). The AEDT uses radar flight track data when available to model trajectories and when unavailable, estimates trajectories based on distributions of cruise altitudes and horizontal track dispersions (dispersed around the great circle path) of existing trajectory data. This method provides a high degree of detail but relies on an expansive set of input data, much of which comes directly from within the FAA and is not freely available. A similarly intricate model is EUROCONTROL's Advanced Emission Model (AEM), which is designed to assess the impact of future regulatory policy options and trends on aircraft fuel burn, emissions, and noise (Whiteley, 2018). While the aforementioned high-fidelity models rely on aircraft performance data from EUROCONTROL's Base of Aircraft Data (BADA) (Nuic et al., 2010), a separately developed performance model from Lissys Ltd. (Lissys Ltd, 2008) is also widely used. The output of the commercial Piano-X model from Lissys has been used for calculating flight-specific emissions (ICAO, 2017) and global carbon accounting (Graver et al., 2019; Winther and Rypdal, 2019). An integrated assessment model from Dray (2018) utilizes Piano-X for investigating the interactions between passengers, airlines, airports, and other system actors. Piano-X, like the AEDT model, is only available with a paid license, and while no purchase is necessary for the use of the AEM model, a license is still required.

Efforts to develop methods for global fuel burn estimation with more publicly available resources have resulted in satisfactorily accurate models. However, as with many of the above mentioned models, the computational complexity of these remains high. Use of such models may require supercomputers for simulations of flight movements of even single years (Wasiuk et al., 2015). This problem becomes more severe as the scope of simulations scales to larger objectives such as multi-year scenario modeling.

Yanto and Liem (2018) developed a method to drastically reduce the computational cost of fuel burn modeling while maintaining estimation error of less than 6% when evaluated against reported fuel volumes from three different airlines. Implementation of this method for U.S. airlines was made possible by the availability of payload data provided by the Bureau of Transport Statistics database of the U.S. Department of Transportation (USDOT). However, as corresponding data is not readily available outside the U.S., the extension of this method to global aviation is challenging.

The goal of this work was to create a model with a minimum of required variable input data and computational cost while maintaining a high level of modeling accuracy. We therefore combine and build upon the existing approaches of generalized flight modeling (Wasiuk et al., 2015) and model order reduction (Yanto and Liem, 2018) in order to create a model capable of simulating global fuel consumption for multiple years and under different scenarios with high computational efficiency. As a result, we propose the *Fuel Estimation in Air Transportation (FEAT)* model: a two-component framework in which (1) a high fidelity flight profile simulator based on BADA aircraft performance models is used to derive (2) a reduced order fuel burn approximation model where aircraft type and great circle distance, trigonometrically derived from an origin-destination airport location pair, are the sole inputs. The reduced order model (2) takes the form of a simple quadratic regression function based on simulated flights from the high fidelity model (1), whereby the aircraft state is continuously evaluated along the flight trajectory using physical equations. Using this combined approach, the computational limitations on multi-year scenario modeling of the Wasiuk et al. (2015) method are overcome without the necessity for route-specific payload data as is required with the Yanto and Liem (2018) method.

The following section presents a description of the two-component modeling framework as well as the derivation of generalized inputs for key modeling parameters. In Section 3, the modeling accuracy is reviewed and computational efficiency is demonstrated. Finally, Section 4 includes final conclusions.

2. Method

The *Fuel Estimation in Air Transportation (FEAT)* framework is comprised of a high fidelity and a reduced order model. Fig. 1 gives an overview on the core FEAT elements. The high fidelity model takes a set of data as input, generates a flight profile, and calculates the fuel needed for that specific flight (see left panel in Fig. 1). A series of simulation points for different flight distances, generated with the high fidelity model, are fitted via ordinary least squares regression, as seen in the center panel in Fig. 1. This model order reduction allows for a simple fuel burn calculation with great circle distance and aircraft type as sole inputs. The fitting parameters per aircraft type, derived in the model order reduction step, can be applied to global flight schedules (see right panel in Fig. 1). The fuel burn per route can then be calculated with high computational efficiency using a vectorized operation. Summing the total fuel consumption per route yields the global fuel burn of one entire year of aircraft movements.

The FEAT high fidelity model introduced in the following section is based on BADA aircraft performance coefficients and procedures (e.g. lift coefficients, flight envelope, climb speed, etc.). While aircraft performance is dictated by these aircraft coefficients, the flight profile generation is dictated by an energy balance equation and a set of simulation procedures. Section 2.1 describes the modeling logic used to generate these flight profiles with a balance of computational speed and precision. The result is a flight profile simulator with substantial flexibility in the selection of aircraft performance and procedural parameters that can be used to estimate fuel consumption of a flight operated between an airport pair with a given aircraft type.

By defining aircraft performance and efficiency parameters generalized for the commercial aviation sector, this flight profile simulator can be leveraged to derive a reduced order fuel consumption model capable of approximating global fuel burn from over 100 aircraft types and millions of flights within milliseconds. The FEAT model order reduction method outlined in Section 2.2

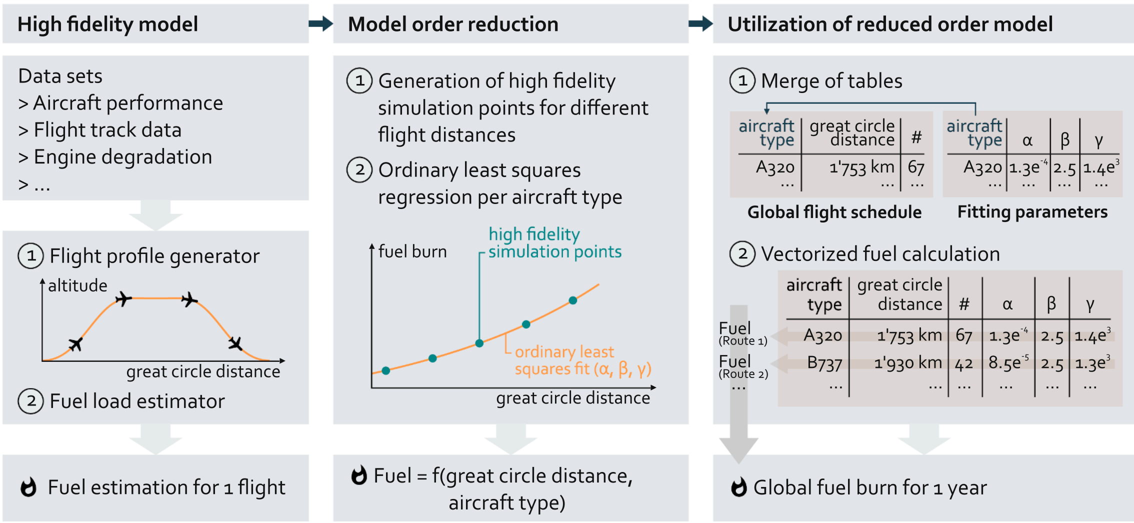

Fig. 1. Overview on the Fuel Estimation in Air Transportation (FEAT) framework: The left column depicts the high fidelity model (see Section 2.1), the center column shows the model order reduction technique (see Section 2.2), and the right column how the reduced order model can be utilized to calculate global fuel burn of all flights scheduled in an entire year (see Section 2.2.5). In the right column, the global flight schedule includes the number of flights per aircraft type-airport pair tuple (while the latter is expressed as the great circle distance). α, β and γ represent the aircraft type-specific parametrizations of the quadratic regression from the model order reduction (see graph in center column).

describes how these generalized parameters are derived with the help of global aircraft fleet data and radar flight track data and implemented for efficient global fuel and CO_2 emissions estimation.

2.1. FEAT high fidelity simulator

The BADA model is based on the total energy model (TEM) of an aircraft, in which the rate of work done by forces acting on the aircraft is equated to the rate of increase in potential and kinetic energy (Mouillet, 2019).

$$(Thr - D)\cdot V_{\mathrm{TAS}} = mg_0\frac{dh}{dt} + mV_{\mathrm{TAS}}\frac{dV_{\mathrm{TAS}}}{dt} \tag{1}$$

The symbols are defined as follows:

- Thr: thrust acting parallel to the aircraft velocity vector
- D: aerodynamic drag
- V_{TAS}: true airspeed
- m: aircraft mass
- h: altitude
- $\frac{d}{dt}$: time derivative
- g_0: gravitational acceleration

Aerodynamic drag is determined from pairs of BADA drag coefficients provided for each flap configuration. One coefficient defines the constant drag component and the other defines the quadratic relationship to the lift coefficient, which is itself calculated assuming level flight (Mouillet, 2019). From the TEM, any one of the three variables, thrust (Thr), speed ($VTAS$), or rate of climb or descent (ROCD, $\frac{dh}{dt}$), can then be determined with knowledge of the other two. During the approach and landing phases of the flight, a standard glide slope of 3° combined with the BADA speed schedule is used to determine aircraft thrust (Kim et al., 2005). In all other phases, the BADA thrust and speed schedules dictate the ROCD of the aircraft.

2.1.1. Flight mission simulation

An overview of the method used to simulate a flight mission with a given distance is outlined in Fig. 2. The mission is divided into 8 stages: taxi-out, take-off, climb, cruise, descent, approach, landing, and taxi-in. Fuel flow rates during the taxi-out, take-off, and taxi-in phases are determined from engine test data supplied in the ICAO Engine Emissions Databank (EED) for jet aircraft (EASA, 2019) and the Swiss Federal Office for Civil Aviation (FOCA) database for piston aircraft engines (FOCA, 2019). For turboprops and all other aircraft that could not be matched to ICAO or FOCA database engines, fuel flow for the taxi and take-off phases were derived from BADA performance coefficients.

While the durations and fuel flow rates of the taxi and take-off phases are constant, those of the climb, cruise, descent, approach, and landing phases are determined using the TEM and BADA performance coefficients. These phases are separated into discrete

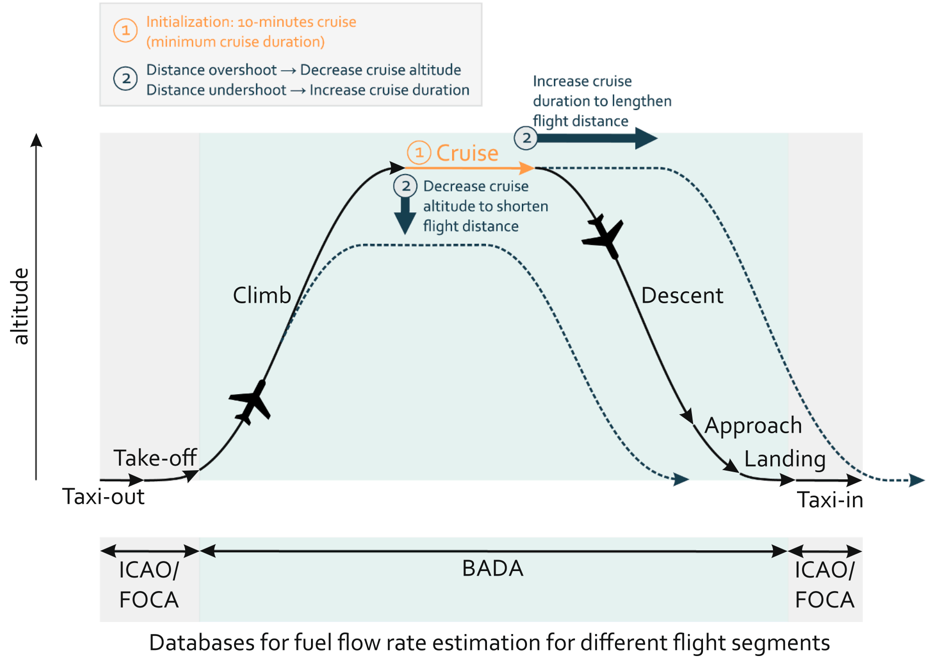

Fig. 2. Flight profile generation procedure and flight path segmentation. Initialization of a 10-min cruise duration, followed by iterative adjustments of cruise duration or altitude until the modeled flight distance equals the target mission distance. The databases for fuel flow rate estimation refer to the ICAO Engine Emissions Databank (EED) for jet aircraft (EASA, 2019), the Swiss Federal Office for Civil Aviation (FOCA) database for piston aircraft engines (FOCA, 2019), and the Base of Aircraft Data (BADA) from EUROCONTROL (Nuic et al., 2010).

segments at which the calculations of aircraft speed, drag, thrust, ROCD, mass, altitude, and flight time are utilized to update the ground-track distance covered by the aircraft. Because aircraft state at each flight segment is determined using the TEM, the effects of any adjustments to aircraft mass, aerodynamics, engine efficiency, or procedural parameters on the flight profile and resulting fuel consumption are captured in the flight profile (e.g. a higher aircraft mass would result in a lower ROCD during climb and higher drag during cruise, resulting in higher fuel consumption).

The change in aircraft mass during the airborne phases of the mission is dependent on fuel consumption, which is in turn related to the mass-dependent performance of the aircraft. Thus, the flight profile from the beginning of climb through the landing phase must be iteratively computed until the target mission distance is achieved. In the first profile iteration, a flight profile is generated with a standard climb to the BADA-derived maximum cruise altitude, a 10-min level cruise (minimum cruise duration), and an immediate descent to landing. The distance traveled during this profile is then compared to the target mission distance. The residual distance is subsequently used to estimate the cruise altitude reduction required to shorten the simulated flight distance if the target mission distance was overshot or to estimate the cruise duration increase necessary to lengthen the simulated flight distance if the target distance was undershot (see Fig. 2). New profiles are generated with the applicable changes iteratively until the residual distance is reduced to less than 1 km, at which point the profile is considered a solution.

The fuel burn for the airborne phase of a flight is subsequently calculated by summing the product of the fuel flow rate and flight time of each segment. The fuel consumed during the taxi and take-off phases are then added to determine the total flight mission fuel consumption. A more detailed description of the mission simulation algorithm and associated flight modeling assumptions is supplied in Appendix B.

2.1.2. Take-off weight estimation

Some fuel burn models use a static aircraft mass for modeling flights (Sheng et al., 2015; FAA, 2017). For example, a reference BADA mass, equal to approximately 70% of the way between the minimum and maximum mass provided for each supported aircraft, can be taken (Poles, 2009). However, aircraft mass has a considerable effect on fuel consumption. Thus, in order to reflect aircraft performance more accurately, a more appropriate method for estimating aircraft take-off weight (TOW) is utilized. The TOW is calculated as follows:

$$m_{\text{TOW}} = m_{\text{OEW}} + m_{\text{payload}} + m_{\text{fuel}}, \tag{2}$$

where m_{OEW} is the aircraft operating empty weight (available in BADA), m_{payload} is the mass of all passengers plus cargo, and m_{fuel} is the mass of the fuel on board. The payload mass is estimated from passenger occupancy and cargo load as described in Section 2.2.4. The fuel load calculation is based on standard airline procedures and is comprised of trip, contingency, destination alternate, and reserve fuel (Wild, 2019). The trip fuel fuel depends on the aircraft performance during the flight profile, which in turn depends on the mass of fuel carried on board. Thus, flight missions are simulated iteratively to determine the amount of trip fuel required for the mission distance. The details of this procedure are included in Appendix G.

2.2. FEAT model order reduction

The profile generation framework, together with the fuel load estimation procedure, enables rapid estimation of fuel consumption for a flight with a given mission distance. It provides a high degree of detail and flexibility and is itself a useful tool for evaluating fuel burn and aircraft behavior for individual flights.

While simulation of all flight routes globally in a given year is possible, doing so requires considerable computational power. Thus, modeling of multiple years and multiple scenarios of air traffic, fleet, or operational changes in this manner would incur prohibitively high CPU hour costs. In order to rapidly estimate global aviation fuel consumption, it is possible to represent the fuel burn performance of a single aircraft type by implementing generalized operational and performance parameters. By approximating payload, engine degradation, and flight route inefficiencies, the flight simulator can be used to derive a simple distance-fuel burn relationship for each aircraft type that can be applied to a global aircraft movement inventory. Approximations are possible by leveraging global flight movements data from OAG Aviation Worldwide Limited (2019), jet aircraft fleet data from Planespotters (2019), and radar flight track data from AirNav Systems (2019).

2.2.1. Flight movements data

Data on global flight movements from scheduled services was purchased from OAG Aviation Worldwide Limited (2019) for the year 2018. The data set contains all commercial flights that were scheduled in the respective year, resolved by number of flights per specific route (uniquely defined by an origin-destination airport pair and an aircraft type). It does not contain general aviation. Pre-processing of the data set included filtering out invalid routes (with excessive great circle distance for given aircraft type), filtering routes performed by military aircraft, merging duplicate aircraft types and airports, and aligning the aircraft types used by OAG with the aircraft types specified in the global aircraft fleet database from Planespotters (see Appendix D). Details on all performed pre-processing steps can be found in Appendix E. Of the 38,086,735 flights supplied in the 2018 OAG data, just 0.38% were filtered during pre-processing and the remaining 37,941,207 flights were used for analysis. The 133 aircraft types remaining after mapping and filtering make up the complete set used for global fuel burn modeling.

2.2.2. Aircraft fleet data

Information on the global aircraft fleet was provided by Planespotters (2019) as a snapshot of the fleet as of 03.07.2019. It contains aircraft hull specifications (type, manufacturer, build date, number of engines, engine type, number of seats) as well as operational information (operator, current status, configuration, etc.). From the raw data set, only in-service aircraft (active and stored) operated by airlines were selected. Missing aircraft configurations (i.e. passenger, freight, or combination carrier) were imputed from the part of the data where this information was given, using statistical and machine learning approaches. Only passenger aircraft were considered subsequently. Finally, the status of the data set was reset to the end of 2018 (to make it aligned with the OAG data). 28,411 aircraft remain in the final fleet database. Further details on the pre-processing can be found in Appendix D. This includes a documentation of all pre-processing steps and the resulting effect on the number of aircraft considered, and further statistical analyses of the aircraft age, status and operators.

The average seat capacity for each modeled aircraft type was derived from the final aircraft fleet database. For aircraft types not present in Planespotters (mainly regional aircraft), seat capacities were obtained from online specifications of the respective aircraft types.

2.2.3. Flight track data

Using Automatic Dependent Surveillance-Broadcast (ADS-B) aircraft flight track data, it is possible to derive flight route inefficiency patterns for different categories of flights by comparing the flight track length to the great circle distance between the start and end points. Aircraft are likely to spend more time in holding patterns above destination airports when air traffic is high, resulting in a greater deviation from the great circle path between the origin and destination airport. Due to seasonal variations in air traffic, almost twice as many passengers are transported by aircraft during the month of August as in the month of January in some regions of the world, such as the EU (Eurostat, 2019). Thus, to capture the behavior of aircraft movements under the widest range of possible operating conditions, ADS-B flight data for the fourth weeks of January and August, 2018, was purchased from AirNav Systems (2019). The data sets included the following information: callsign, mode-s hex code, aircraft registration, aircraft type, departure airport code, arrival airport code, timestamp, latitude, longitude, ground speed, heading, altitude, and ROCD. The distance traveled between each recorded point was approximated by the great circle distance between the coordinate locations and the total flight path distance was calculated by summing these values for the entire flight.

After cleaning and filtering (see Appendix F), the resulting set of flight track data (corresponding to 211,773 flights) was used to approximately relate the great circle distance between a flight's starting and ending point to the flight distance traveled between them. A description of the relationship and its implementation is included in the following section.

2.2.4. Generalized aircraft parameters

In order to leverage the OAG flight movements data set to estimate global fuel consumption, a single representative reduced order model is created for each aircraft type. Aircraft-specific average payload and engine degradation values are determined using the flight movements and fleet data. A generalized distance correction derived using the radar flight track data is used universally for all aircraft.

Aircraft take-off weight, has a particularly pronounced impact on the amount of fuel consumed during climb on short haul flights due to the simple energy balance and an additional effect on long haul flights due to lift-induced drag. Uncertainty quantification of the FAA's AEDT indicated that 10% variation in departure weight had an impact of approximately 5% on fuel burn (FAA, 2017). While the reduced order model precludes the specification of any particular flight-specific TOW, average passenger and belly cargo load factors can be combined with aircraft seat capacities to approximate average payload.

With the seat capacity for each type estimated from the aircraft fleet database, the number of on board passengers is modeled using an average load factor of 81.9% for 2018 (IATA, 2019). Many airlines utilize extra space in the belly of their larger jet aircraft to transport freight as a source of additional revenue on passenger flights. The amount of belly cargo carried by each aircraft type is approximated using an average passenger-to-freight factor, which represents the ratio of the mass of passengers (plus their luggage) to the total payload mass (including freight). A global average passenger-to-freight factor of 85.1% was obtained by taking a weighted average of individual ICAO route group factors (Graver et al., 2019). The factors were weighted by the proportion of global flight kilometers performed within each route group according to the OAG movements data. The mass of each passenger plus associated luggage is taken to be 100 kg (ICAO, 2009). From this value, the payload of each aircraft is calculated using the average number of seats, load factor, and passenger-to-freight factor where applicable.

Aircraft inefficiencies due to engine deterioration and fouling are another important modeling consideration. Due to airborne contaminants like sand, soot, water, or insects, the surface roughness of turbine blades increases. This deterioration induces thicker boundary layers and decreases the engine's efficiency (EcoPower, 2020). Engine deterioration leads to regular overhauls when the resulting specific fuel consumption increase is around 2-4% (IPCC, 1999). Thus an aircraft's fuel burn performance depends not only on its age, but also on the overhaul interval. The influence of these engine degradation effects are implemented by combining fleet age averages and degradation rate to determine an average fuel efficiency deficit for each aircraft type.

In October 2019, we conducted an expert interview with Mr. Urs Glarner, Sr. Field Representative at the Customer Service of Pratt & Whitney/ IAE International Aero Engines (Glarner, 2019). Using his insights on usual engine degradation and restoration measures, we derived a first-order approximation of the expectable loss in engine efficiency over time for the average medium- and long-haul aircraft. The resulting logarithmic engine degradation, δ, expressed as the percentage decrease in engine efficiency dependent on the age (in years), t, of the aircraft was found to be:

$$\delta(t) = -1.28log(t+1) \text{ for medium-haul aircraft} \tag{3}$$

$$\delta(t) = -1.34log(t+1) \text{ for long-haulaircraft} \tag{4}$$

Both results and underlying assumptions are provided in the Appendix H. We correct the fuel consumption that is calculated in the fuel burn model assuming a new engine, F_{new}, by the efficiency loss per aircraft type that is present in the 2018 fleet using the following equation:

$$F_{corr} = \frac{F_{new}}{100 - \delta(\bar{t})} \tag{5}$$

with δ being the engine degradation factor for the average age, $\bar{t}$, of the respective aircraft type derived from the aircraft fleet data. Aircraft are classified as medium- or long-haul according to their average great circle distance, which we compute using the flight movements data (great circle distance weighted by the frequency of each route). The classification demarcation is set at 4,000 km.

A final key consideration for estimating fuel consumption is flight route inefficiencies. Aircraft rarely fly direct great circle paths from departure to destination airport but rather fly prolonged flight tracks due to maneuvering and air traffic management (ATM) inefficiencies. The Intergovernmental Panel on Climate Change (IPCC) suggests that alleviating ATM inefficiencies could reduce fuel burn by between 6% and 12% (IPCC, 1999), demonstrating the importance of including such inefficiencies in fuel burn modeling.

In order to leverage ADS-B data, the following linear relationship was derived:

$$d_{fp} = a \cdot d_{gc} + b, \tag{6}$$

where d_{fp} is the flight path distance and d_{gc} is the great circle distance between the start and end points. The set of filtered and cleaned AirNav Systems flights was used to calculate parameters a, 1.0387, and b, 40.5, via ordinary least squares regression (see Appendix I). Eq. 6 is then used to adjust the target mission distance provided to the flight profile simulator in order to incorporate the effects of average flight route inefficiencies when simulating a mission.

2.2.5. FEAT reduced order model implementation

The reduced order distance-fuel burn relationships used to estimate global fuel consumption from the flight movements inventory are derived from a set of simulated flights for each aircraft type. Using the described payload, engine degradation, and distance correction generalizations, 25 flights over a range of mission distances were simulated using the high fidelity fuel burn model. The simulation distances were linearly spaced between a minimum value and maximum mission distances found for each aircraft in the OAG dataset. The minimum value was the greater of 200 km or the minimum mission distance found for the aircraft in the OAG dataset. Below 200 km, the high fidelity model is often unable to accurately generate realistic flight profiles. Simulation of such flights would therefore inappropriately skew the reduced order model derivation. The reduced order distance-fuel burn relationship takes the form of a quadratic regression function:

$$F_i = \alpha_i \cdot d_{\mathrm{gc}}^2 + \beta_i \cdot d_{\mathrm{gc}} + \gamma_i, \tag{7}$$

where the fuel burn, F_i, of a flight is estimated using the great circle distance, d_{gc}, between the origin and destination airport, and the parameters, α_i, β_i, and γ_i, are calculated using ordinary least squares regression for each aircraft type, i.

Each route in the processed OAG dataset is uniquely defined by an origin-destination airport pair and an aircraft type. With the mission distance calculated as the great circle distance between the airport pair, the aircraft-specific reduced order function is used to estimate the fuel consumption of each flight along that route. The total fuel consumption by a route for a given year is then calculated by multiplying with the number of performed flights on that route. Global aviation fuel consumption is estimated by taking the sum of fuel consumption on all routes. This procedure is depicted in the right panel of Fig. 1. There are a number of assumptions and simplifications that may effect the accuracy of such estimates and they must be considered:

- No military flights were modeled. While military fuel consumption is estimated to be in the range of 10% of the total emissions from aviation (Wilkerson et al., 2010), the modeling of military aircraft operations is beyond the scope of this work due to restricted access to aircraft and movements data.
- Unscheduled flights were not modeled. While unscheduled flights can account for over 9% of flights in regions such as Western Europe (Kim et al., 2007), estimation of fuel burn from these flights is outside the scope of this work due to limited availability of aircraft and movements data.
- All aircraft were modeled as passenger aircraft. While some freighter operations were captured in the OAG data set, OAG noted that the coverage of those flights was virtually non-existent. The global average freight load factor in 2018 was just 49%, which suggests aircraft configured as freighters typically carry lesser payloads than passenger aircraft. Thus, modeling freighter aircraft as passenger aircraft is likely to result in an overestimation of fuel consumption for those flights. The sensitivity of fuel estimation to load factor can be found in Appendix C.
- The average seat number for each aircraft type was used to calculate the passenger payload.
- Belly freight mass was included for aircraft in the ICAO-specified medium, heavy, and jumbo wake categories only. Smaller aircraft such as small jets, turboprops, and piston aircraft do not carry belly freight (Wild, 2019).
- The average passenger-to-freight factor was used uniformly for all flights. In reality, this factor depends largely on the flight route and operating airline. A 10% change in passenger-to-freight factor induces a 1-3% change in fuel consumption for most flights. The sensitivity of fuel estimation to passenger-to-freight factor is explored in more detail in Appendix C.
- The flight distance adjustment simply extends the mission distance of a flight. By implementing the adjustment this way, the distance adjustment is effectively added to the cruise phase of the flight. In reality, much of the flight route inefficiencies such as maneuvering and holding occur during the other flight phases and at lower altitudes. As per-kilometer fuel economy at reduced altitudes is lower, adding the distance adjustment to only the cruise phase most likely leads to an underestimation of the fuel impact from flight route inefficiencies.
- Fuel consumed by auxiliary power units (APUs) during ground operations of aircraft was not considered. APU fuel consumption is estimated to be in the range of 1% of total fuel consumption of an aircraft, but is subject to a high degree of uncertainty (IPCC, 1999).
- All jet aircraft are assumed to burn Jet A-1 fuel and all piston aircraft are assumed to burn Avgas, where the CO_2 emission indices are taken to be 3.16 $kg\ CO_2/kg\ fuel$ and 3.10 $kg\ CO_2/kg\ fuel$, respectively (ICAO, 2019; Shell Aviation, 2014).
- Wind effects on fuel burn were neglected due to the uncertainties in flight plans and wind conditions (Sheng et al., 2015). Airlines usually try to harvest tail winds, in particular from jetstreams. While the overestimation of fuel burn on specific flights can be high, "the overall overestimation is around 1%." (Sheng et al., 2015). This is confirmed by a study from Simone et al. (2013) who find an overestimation of 0.6%. A detailed modeling of wind effects requires spatially and time-resolved information on wind conditions, particularly for high altitudes.

3. Results and discussion

The efficacy of the proposed reduced order fuel consumption model depends on its modeling accuracy. Furthermore, it is important to understand what the sources and impact of modeling errors are. Keeping these facts in mind, the reduced order model can be leveraged to estimate fuel consumption and explore changes in aviation operational and technological performance parameters. Thus, in this section, we discuss the accuracy, sensitivity, efficiency, and results of the *Fuel Estimation in Air Transportation (FEAT)* framework.

3.1. Accuracy of FEAT reduced order models

The reduced order model regression curves for all modeled aircraft are shown in Fig. 3. The complete set of regression coefficients can be found in Appendix M. The wide deviation in the curves seen in Fig. 3 demonstrates the importance of selecting the appropriate aircraft model for fuel consumption estimation. For a 2,000 km flight, fuel consumption varies from around 1 ton to 10 tons for jet aircraft with less than 150 seats and can reach more than 30 tons for jet aircraft with more than 150 seats. The bottom right plot is obtained by dividing the fuel consumption for a flight by the average seat capacity for the aircraft type as derived from the Planespotters data set. Thus, it does not reflect the exact fuel consumption per passenger carried, but rather gives a visualization of the relative performance of the 4 aircraft categories.

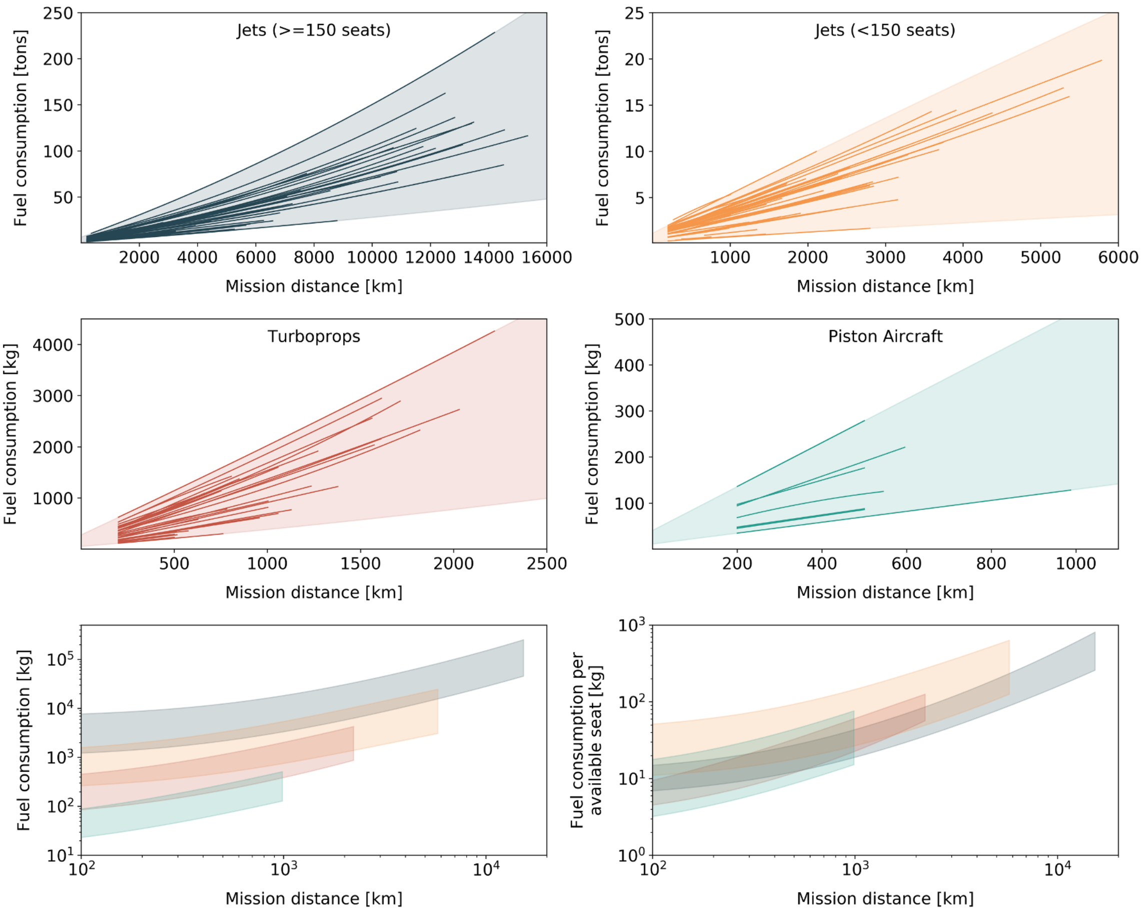

Fig. 3. Reduced order regression curves for jet aircraft with at least 150 seats (top left) and less than 150 seats (top right). The curves for turboprops and piston powered aircraft are shown in the left and right middle plots, respectively. The bottom left is a reproduction of the shaded areas of the plots above, in which the uppermost and lowermost reduced order curves for each aircraft category are displayed on a log-log plot. The bottom right illustrates the range of efficiencies for each category in the form of fuel consumption per passenger on a log-log scale.

All curves in Fig. 3 are nearly linear and roughly 80% of them have upward curves, with the remaining 26 aircraft having negative quadratic term coefficients. An upward curve is expected from the effect of the fuel load: for longer missions, the mass of fuel carried on board is higher, which increases the fuel burned during take-off (due to basic energy balance) and cruise (due to lift induced drag). However, for long missions, aircraft mass is limited by a specified maximum take-off weight (MTOW). Thus, for missions longer than a critical distance, the effect of increasing TOW disappears. This effect and others are discussed in Appendix C.

By utilizing a quadratic function instead of a simple linear relationship between mission distance and fuel burn, some of the subtle characteristics of the high fidelity model can be incorporated (see Appendix C). Nonetheless, the reduced order model is still an approximation and the precision must therefore be reviewed. The coefficient of determination (R^2) for the reduced order regression functions with respect to the simulated high fidelity samples (based on 25 simulation points generated by the high fidelity model) of all modeled aircraft is shown in Fig. 4. The mean R^2 value of all 133 aircraft is 0.9997 and all aircraft have R^2 values greater than 0.997 which suggest universally good fit of the reduced order models to the high fidelity simulated flights. Reasons for variation in model fits are discussed in Appendix C.

3.2. Aggregated fuel consumption modeling error

While the coefficient of determination describes the goodness of fit of the reduced order models relative to the high fidelity simulation points across the whole range of mission distances, the reduced order model must also be evaluated against real flight movements, according to its intended application. Thus, 1,000 routes were randomly selected from the 2018 OAG flight movements data set and the CO_2 emissions of each were estimated first by directly simulating the flight with the high fidelity model and then by implementing the reduced order model. The error of the latter estimate with respect to the former was calculated for each. The resulting distribution of the modeling error for single flights (N = 1) shown in the top plot of Fig. 5 has a mean of just -0.09%. The 95% confidence interval of the modeling errors reveals a noticeable skew toward underestimation.

Fig. 4. The coefficient of determination (R^2) for the reduced order regression functions derived for each modeled jet, turboprop, and piston aircraft based on 25 simulation points generated by the high fidelity model. All aircraft fuel burn functions have R^2 values greater than 0.997. The 7 aircraft types for which the bars have hashes make up over 60% of flight route kilometers in the 2018 OAG flight movements data set.

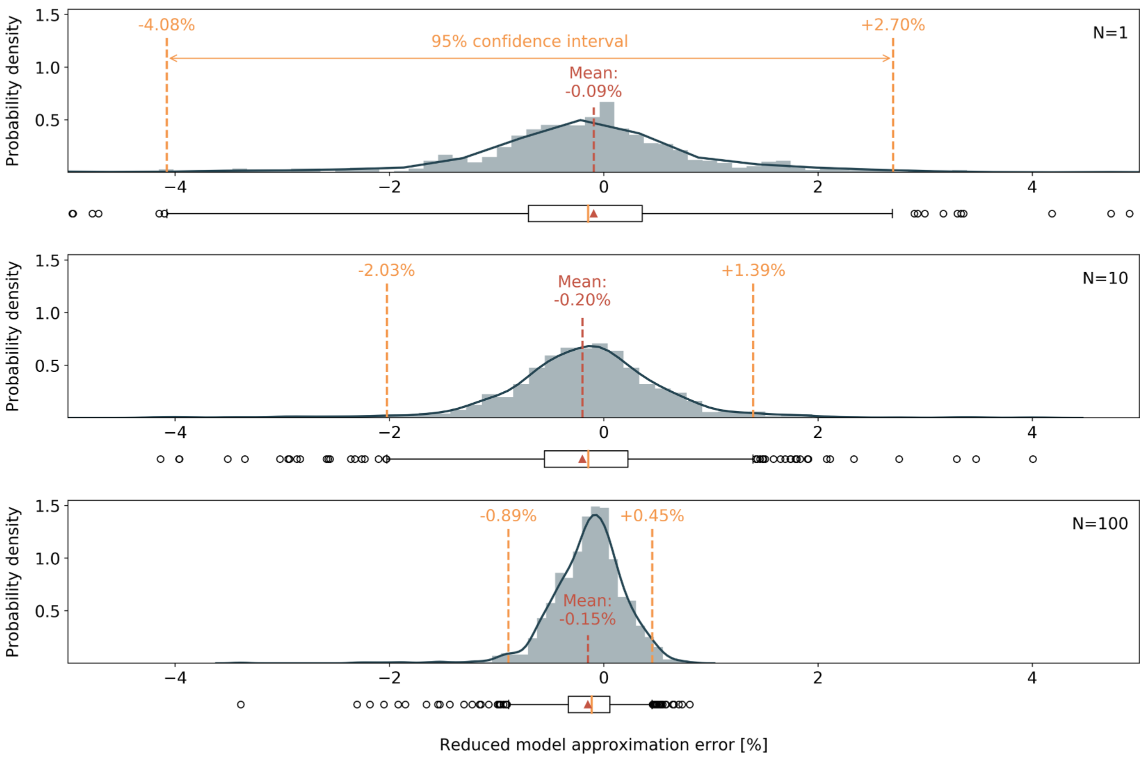

Fig. 5. Distributions of fuel burn estimation error of the reduced order models relative to that of the high fidelity flight simulator. 1,000 trials were performed by randomly selecting 1 (top left), 10 (bottom left), or 100 (bottom right) routes from the 2018 OAG flight movements data set and estimating the aggregated fuel consumption with each method. The box plot whiskers span the 95% confidence interval and the boxes span the interquartile range. The red triangle depicts the average error, and the vertical, orange line in the box plot the median error. (For interpretation of the references to color in this figure legend, the reader is referred to the web version of this article.)

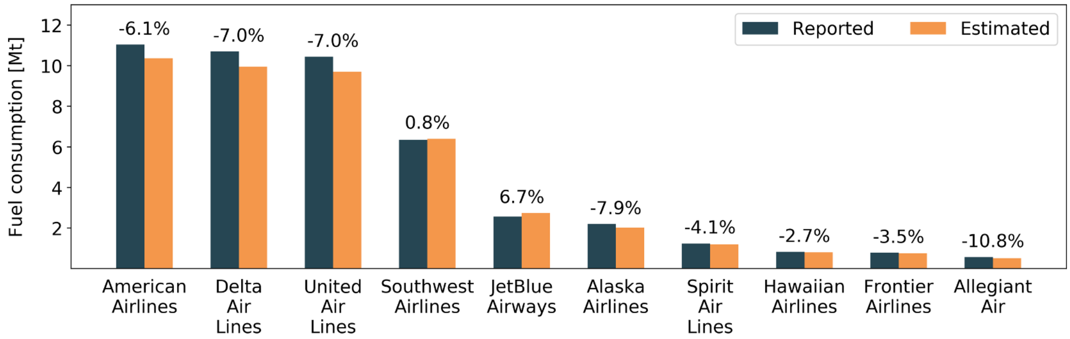

Fig. 6. Fuel consumption of the ten largest U.S. airlines in 2018 as reported by the U.S. Department of Transportation Bureau of Transport statistics and estimated using reduced order aircraft fuel burn models. The percentage error on top of the bars represents the difference between the reported and the estimated values.

The farthest outliers, which skew the distribution toward larger underestimations, correspond to routes with great circle distances around or below 200 km. Estimation with the reduced model for flights less than 200 km occurs via extrapolation of the regression function below the lowest simulated mission distance, which is no less than 200 km (see Section 2.2.5). This extrapolation does not accurately capture the behavior of aircraft fuel consumption for low mission distances due to cruise altitude effects (see Appendix C) and and tends to lead to high approximation error relative to the high fidelity model. As routes with great circle distances less than 200 km make up only about 0.5% of flight kilometers in the 2018 OAG data set, the overall effect of these error outliers is small.

As the intended application of the reduced order modeling method is global fuel and emissions estimation, the overall effect of the model order reduction on aggregated CO_2 emissions estimates is evaluated. A set of ten routes (N = 10) was randomly sampled from the 2018 OAG flight movements data set and the aggregated CO_2 emissions were estimated with the FEAT reduced order and high fidelity models as before. The flight movements data set was resampled with replacement and the associated errors in aggregated CO_2 emissions were calculated 1,000 times. This procedure was repeated for a set of 100 routes (N = 100). The middle (N = 10) and bottom (N = 100) plots in Fig. 5 show the corresponding error of the reduced order models. For aggregated CO_2 emissions estimates with just 100 routes, the 95% confidence interval of the approximation error is from -0.89% to 0.45%. While some aircraft types can be approximated more precisely with the reduced order quadratic function than others, the total error when estimating aggregated fuel consumption on the scale of yearly flight movements (hundreds of thousands of routes) is sufficiently low.

To validate the accuracy of our fuel consumption estimation, it is crucial to compare our results to reported fuel consumption values. However, there is a lack of open data; we found the U.S. Department of Transportation Bureau of Transport Statistics (BTS) T-100 flight segments database (USDOT, 2018) to be the most comprehensive open data set on reported fuel consumption figures publicly available. Therefore, the reduced order aircraft fuel burn models were used to estimate total fuel consumption of the 10 largest U.S. airlines in 2018 from the BTS data set. Fig. 6 compares the estimated fuel consumption to the reported fuel consumption for each airline (USDOT, 2019). For all 10 airlines combined, the reduced order fuel burn models underestimate the reported fuel consumption by 4.8%. The potential sources of this error include the numerous assumptions and simplifications listed in Section 2.2.5 and Appendix B. However, a few are likely to have a bigger impact than others. In particular, the 81.9% average load factor used for all flights when modeling was likely lower than the average load factors of these U.S. airlines in 2018. For example, the three biggest airlines, American Airlines, Delta Air Lines, and United Air Lines had load factors of 83%, 86%, and 83%, respectively, in 2018 (MIT, 2020). Other reasons for the fuel underestimation include the use of optimal cruise altitudes and continuous descents in the model, whereas in reality, aircraft may spend considerable time flying at lower altitudes due to airline procedures or air traffic control instructions. Estimated fuel consumption by JetBlue Airways stands out as the only case of significant overestimation. This can be explained by the fact that the airline did not have any significant air cargo operation in 2018 (Coker, 2019). Thus, by modeling JetBlue operations with reduced fuel consumption models produced with belly cargo included, we overestimate the fuel consumed by flights with passenger aircraft.

The total fuel consumption and CO_2 emissions estimated for 2018 by combining aircraft regression functions with the OAG flight movements data set is 257 Mt of fuel and 812 Mt CO_2, respectively. Of those emissions, 98.9% were from jet aircraft. This estimate includes all validated commercial passenger flights recorded by OAG as well as a small number of freighter flights (see 2.2.1 and 2.2.5). The International Air Transport Association (IATA, 2019) reports CO_2 emissions of 905 Mt for 2018. However, the IATA accounting method includes freighter aircraft operations, which makes a direct comparison more difficult. The International Council on Clean Transportation (ICCT) estimates that 8% of commercial aviation CO_2 emissions result from dedicated freighter operations (Graver et al., 2019). By this measure, the passenger aircraft emissions using the reported IATA value is about 833 Mt, 1.7% higher than our estimate. The ICCT estimate of CO_2 emissions from passenger aircraft (including those carrying belly freight) in 2018, 848 Mt, was calculated based on 37.97 million flights (compared to our 37.94 million flights) using Piano 5, a commercial flight modeling software model from Lissys Ltd. (Graver et al., 2019; Lissys Ltd, 2008). Graver et al. (2019) acknowledged that the model tends to underestimate real fuel burn, so fuel burn per RPK was scaled by a factor of 1.02 to 1.20 for each aircraft. The 4.3% difference in 2018 CO_2 emissions estimated by our model relative to the ICCT value is comparable to the previously mentioned 4.8% fuel burn underestimation relative to the BTS reported fuel volumes.

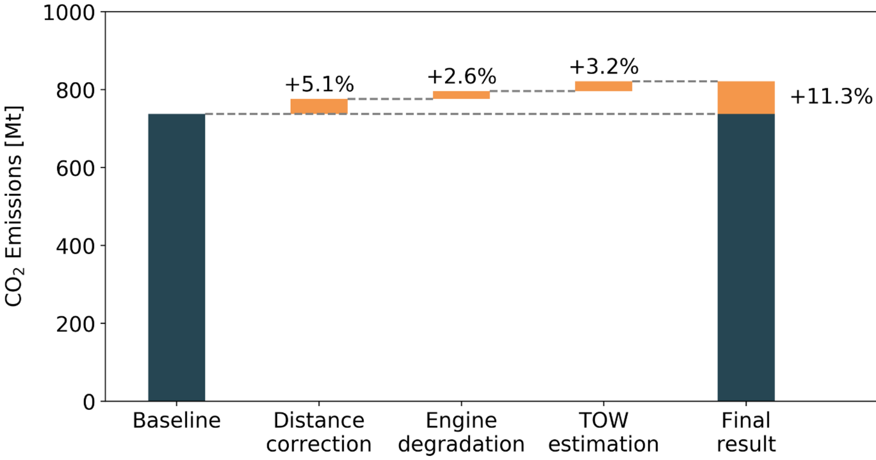

Fig. 7. Effects of key modeling assumptions on global commercial aviation CO_2 emissions estimates for scheduled flight movements in 2018. TOW = Take-off weight.

It is up for discussion which aggregate CO_2 emission values (IATA, ICCT, FEAT) represent reality better. Since the IATA biannual report does not state the origin of its CO_2 emissions value, we compare the methodological approach of the ICCT report with this study's FEAT approach. The ICCT compares their results against the BTS data set, i.e. aircraft operations in the U.S., and adjusts the fuel consumption per aircraft type upward so that the U.S. BTS values are matched. Their scaling factors range "from 1.02 to 1.20 by aircraft class, and averaged 9% across all classes." Undoubtedly, this creates a significant bias towards U.S. operations, e.g. in terms of higher load factors in the U.S. than in other world regions. Accounting for that alone reveals a potential overestimation of global CO_2 emissions by the ICCT. Using an equivalent scaling method to fit the BTS data set would shrink the difference between the emission values from our proposed FEAT method and the ICCT report significantly (note that we are underestimating the BTS fuel volumes by 4.8% and the ICCT volumes by 4.3%). However, FEAT takes a different approach: instead of using mere scaling factors, we refine existing aircraft performance modeling phenomenologically, e.g. by implementing engine degradation factors. This might be a less biased approach in the race for ever-increasing modeling accuracy of global fuel and CO_2 estimation methods. In the end, a comprehensive comparison of different approaches is impeded by the lack of data. A data set on regional fuel sales resolved by airline or aircraft types, similar to the BTS, is considered to be crucial for future model comparisons.

3.3. Modeling parameter impact assessment

There are numerous modeling assumptions listed in Section 2 that can contribute to the CO_2 emissions estimation error. Therefore, key modeling assumptions and their impact on the 2018 CO_2 emissions estimate are investigated. Fig. 7 shows the effect of 3 key modeling components on the estimated CO_2 emissions relative to a baseline case for 2018 using the reduced order modeling method. The baseline case is determined using simplifying assumptions made in many other fuel estimation models: no flight route inefficiencies, no engine degradation, and a reference aircraft TOW (BADA reference mass in this case). Inclusion of the distance correction procedure increases the CO_2 emissions estimate 5.1% above the baseline case. Addition of engine degradation effects and TOW estimation increases the estimate an additional 2.6% and 3.2%, respectively. The listed modeling assumptions have a combined effect of 11.3% on the global emissions estimate relative to the baseline.

While each refinement significantly reduces the magnitude of underestimation by the global reduced order model, the impact from the distance correction is greatest. Inclusion of flight route inefficiencies into the model increases estimation of CO_2 emissions by nearly 40 Mt. A case study by Prats et al. (2019) suggest that fuel inefficiencies attributable to air traffic management are around 7.8%. Another study suggests fuel consumption could be reduced by 11-12% by eliminating delays and terminal area inefficiencies (Ryerson et al., 2014). Given also the suggestion by the IPCC that ATM inefficiencies could reduce fuel burn by between 6% and 12% (IPCC, 1999), it is likely that we underestimate fight route inefficiencies (5.1%) in our model. The inclusion of such modeling assumptions is crucial for improving fuel burn estimates, but exact quantification of key parameters such as flight route inefficiencies, engine degradation, and TOW for use in reduced order aircraft models can be difficult without access to extensive and often proprietary data.

3.4. Computational efficiency

Table 1 gives an overview of the computational time required for key operations with the FEAT high fidelity and reduced order models. As the computational time for full flight simulation is 1-3 s on a single processor, generation of a complete set of 133 reduced order models is possible in a matter of minutes with even modest parallelization.

Deriving the reduced order models using 25 samples for each of the 133 modeled aircraft takes approximately 25 min with 8 processors. If the reduced models are derived from a set of only 3 simulated flights, the reduced order model generation time is

Table 1
Computational time of key modeling operations. A 2.6 GHz processor was used for all computations. Note that 133 aircraft types represent the complete set of aircraft in the global flight movement schedule in 2018. "Simulation points" are calculated using the FEAT high fidelity model.

Computation	Scope	Degree of parallelism	Required time (approximate)
High fidelity model implementation	Single flight simulation	1	1–3 s
Reduced order model generation	1 aircraft, 25 simulation points	1	45 s
	1 aircraft, 5 simulation points	1	10 s
	1 aircraft, 3 simulation points	1	6 s
	133 aircraft, 25 simulation points each	8	25 min
	133 aircraft, 5 simulation points each	8	5 min
	133 aircraft, 3 simulation points each	8	3 min
Vectorized reduced order model implementation	Single year global fuel estimation	1	43 ms

correspondingly reduced by 88%. An investigation of the impact of the number of simulation points used to derive the reduced order models showed only a minor penalty in approximation error using 3 simulation points instead of 25. The mean approximation error of reduced order models derived from 25 simulation points relative to the high fidelity model was -0.17% ($\sigma = 0.93\%$), while the mean error using 3 samples was -0.84% ($\sigma = 1.39\%$), see detailed analysis in Appendix J. In the interest of maximizing accuracy, 25 simulation points were nevertheless used to generate the models used for 2018 fuel and emissions estimates in this report. As there are nearly 200,000 unique flight routes globally, calculating fuel consumption for a single year with this reduced order approach decreases the number of flights that must be simulated by a factor of more than 50 to just 3,325 flights (133 aircraft x 25 simulation points per aircraft to derive the reduced order models). If computational expedience is prioritized, global fuel consumption can be calculated using regression models with as few as 3 simulation points, which reduces the number of simulations by a factor of 500 to just 399 flights (133 aircraft x 3 simulation points).

In the cases of multi-year scenario modeling, the benefit of the model order reduction becomes very clear. Once the reduced order aircraft models are generated, they can be applied to any number of historical or hypothetical flight movement data sets without performing any additional full profile simulations. Calculation of emissions estimates for a single year is accomplished using efficient vector operations by applying Eq. 7 with aircraft-specific reduced model regression coefficients and great circle distance vectors for all routes. Using this approach, Table 1 shows that computation of global fuel and CO_2 emissions estimates for 2018 (corresponding to approximately 38 million flights) was completed in just 43 ms on a single 2.6 GHz processor core. Hence, the complete FEAT modeling framework of (1) creating a high fidelity model per aircraft (3 simulation points each) and (2) estimating global fuel burn and CO_2 emissions using the respective reduced order models takes less than 4 min.

3.5. Model applications

While Yanto and Liem (2018) utilize BADA to derive climb range and fuel correction factors to an otherwise simplistic fuel consumption model based on the Breguet range equation, the implementation of complete BADA-based flight profile simulation in FEAT provides a significantly higher level of modeling detail. With this approach, it is possible to adjust aircraft parameters (e.g. drag coefficient, specific fuel consumption operating empty weight) and incorporate their effects into the reduced order models.

Relative to Wasiuk et al. (2015), FEAT incorporates only a few additional modeling details: flight distance correction, inclusion of cargo, and modeling of some piston aircraft. However, the ability to model a particular flight as accurately as possible was not the objective. In fact, validation of the BADA or related models are the focus of numerous other existing works (Nuic et al., 2010; Oaks et al., 2010; Hadjaz et al., 2012; Pagoni and Psaraki-Kalouptsidi, 2017; FAA, 2017; Dalmau et al., 2020). Instead, FEAT offers a procedure to reduce the modeling complexity for the efficient estimation of global aircraft fuel consumption and CO_2 emissions while simultaneously retaining the modeling flexibility to reflect aircraft performance and operational adjustments on these estimates. In this sense, FEAT's value is derived not from the accuracy of the high fidelity model, but on the ability to efficiently reflect the influence of aircraft performance and operational factors such as aircraft glide ratio or operating empty weight on global commercial aviation fuel consumption and emissions (see Appendix K).

The exceptional efficiency of computing global CO_2 emissions using the reduced order models enables numerous pathways for further investigation of current and future aviation emissions. The sole input to global estimation using the reduced order models (available in Appendix M) is a flight movements data set containing the aircraft type, great circle distance, and frequency of each route. Thus, fleet turnover and flight route projections can be combined to create any number of future flight movement scenarios which together with the reduced order models can be leveraged to generate valuable insights. For example, by utilizing aircraft retirement curves (e.g. from Dray (2013)) and market forecasts (e.g. from Airbus (2019), Boeing (2019), or ICAO (2018)), future aircraft emissions under various assumptions of global aviation development can be easily estimated.

The scope of analysis can also be expanded by utilizing the flexibility of the high fidelity model. The reduced order models developed in this study were generated with load factor, engine degradation, and other input parameters derived from air transport performance data for 2018. Such generalizations do not lead to major modelling accuracy improvements over existing methods, such as those from Wasiuk et al. (2015). However, by adjusting these input parameters, the complex aircraft performance interdependencies captured by the high fidelity model enable efficient investigation of operational and technological improvement scenarios beyond 2018. Each time an aircraft high fidelity model input parameter is changed, a new reduced order model must be

Table 2
Potential analyses of Key Performance Indicators (KPIs) across the CORSIA themes. CORSIA is the Carbon Offsetting and Reduction Scheme for International Aviation from the International Civil Aviation Organization (ICAO).

CORSIA Theme	KPI	Description	Reduced models generation required
Aircraft Technology	Glide ratio	Improvement in aircraft aerodynamics due to advanced wing and body designs as well as retrofits can lead to improvements in aircraft glide (lift-to-drag) ratio	yes
	OEW	Updated aircraft structural designs and use of advanced materials can lead to reductions in aircraft operating empty weight (OEW).	yes
	TSFC	Ultra high bypass turbofans, open rotor concepts, hybrid turbines, and other advanced propulsion technologies can lead to reductions in aircraft thrust specific fuel consumption (TSFC).	yes
Operational Improvements	Load factor	Improved aircraft load factors can limit emissions growth as air travel demand increases by filling more empty seats on existing flights, which enables airlines to transport more passengers without increasing the number of flights.	yes
	ATM	Optimizing aircraft trajectories with advanced air traffic management (ATM) enables aircraft to fly optimally and reduce overall emissions.	yes
	Engine degradation	Shortening engine overhaul and wash intervals limits the fuel efficiency losses from degradation and ageing, which in turn limits emissions.	yes
	Taxi time	Reduction of taxi times can reduce emissions in this phase.	yes
Sustainable Aviation Fuels	Energy carrier	Electrically assisted taxi-in can decrease emissions in this phase, when using renewable electricity.	no
	Energy carrier	Low carbon fuels have a high potential to bring down global emissions from aviation, most prominently e-fuels (from renewable electricity, based on electrolysis), bio-fuels, and solar fuels (from high-temperature thermochemical processes).	no

created according to the process described in Section 2.2.5. While this process is considerably slower than directly utilizing previously generated models, Table 1 shows that it is still very efficient. Three case studies performed using this approach are included in Appendix K.

The flexibility of the high fidelity model and efficiency of yearly CO_2 emissions estimations with the reduced order models can be leveraged together to evaluate decarbonization pathways in aviation. The Carbon Offsetting and Reduction Scheme for International Aviation (CORSIA) is a framework to achieve ICAO's global aspirational goals: (1) to improve energy efficiency by 2% per year until 2050, and (2) to achieve carbon neutral growth from 2020 onwards (ICAO, 2019). Table 2 illustrates how the potential of analyses enabled by these models spans the basket of measures (aircraft technology innovations, operational improvements, and sustainable aviation fuels) central to the CORSIA framework.

Using typical aircraft fuel modeling techniques, multi-year emissions estimation for numerous scenarios of the type described in Table 2 would come at immense computational cost. The *Fuel Estimation in Air Transportation (FEAT)* model order reduction framework thus offers a unique and powerful tool for assessing global aviation decarbonization pathways.

4. Conclusions

In this paper, we combine existing techniques of aircraft flight modeling and model order reduction to develop a framework for efficiently estimating global fuel consumption and CO_2 emissions with a high level of accuracy. The result is the *Fuel Estimation in Air Transportation (FEAT)* framework consisting of a high fidelity and a reduced order model.

The necessity for numerous inputs to estimate fuel consumption that plagues many other models is avoided with our method by utilizing various data sources to derive both aircraft-specific and generic parameters: average seat capacity and engine degradation factors for each aircraft type were derived using a worldwide aircraft fleet data set and generalized flight route inefficiency factors were calculated using a representative set of flight track data. Using these and other simplifications, quadratic regression functions approximating the distance-fuel burn relationship of 133 jets, turboprops, and piston powered aircraft were derived. The functions were shown to approximate the high fidelity flight profile simulator with an error less than $\pm 1\%$ when estimating aggregate fuel consumption for 100 routes with greater than 95% confidence.

The reduced order models and the generalized parameters with which they were derived were validated against airline data from the U.S. Bureau of Transport Statistics. Fuel consumption estimates calculated using the reduced order fuel burn regression functions and flight movement data for the 10 largest U.S. passenger air carriers were just 4.8% less than the reported volumes.

As the fuel consumption modeling order reduction results in simple aircraft-specific quadratic functions with mission distance as the only input, computation time of fuel consumption and CO_2 emissions estimates from global scheduled flight movements is reduced to mere milliseconds. The estimated CO_2 emissions from commercial passenger aviation in 2018 using flight movements data from OAG was 812 Mt CO_2. This represents a 1.7-4.3% lower estimate relative to figures reported by IATA and ICCT. In the discussion of this work, we highlight the benefits of our approach compared to existing models and explain the differences in total CO_2 emission values.

An impact assessment of modeling assumptions was performed using a set of widely used modeling assumptions as the benchmark. Results suggest that the inclusion of take-off weight (TOW) estimation and engine degradation effects can have an impact on estimates in the range of 3%, whereas inclusion of flight path inefficiencies has a slightly higher impact of roughly 5%.

While the model order reduction method described in this paper was shown to perform sufficiently well for global fuel and emissions estimates, improvements could be made with the inclusion of additional data. A deeper analysis of ADS-B flight track patterns or more accurate data in general would lead to a more precise representation of flight path inefficiencies and may increase accuracy of fuel and emissions estimates. Furthermore, additional data regarding aircraft passenger and freight load factors would be very beneficial for refining the estimation of aircraft TOW.

In the end, the computational efficiency of the reduced fuel burn model provides a viable method for estimating current global fuel consumption rates and offers a tool for predicting future trends as well. Thanks to the ease by which this reduced model can be derived from the high fidelity model, various multi-year policy, technology, and market-based scenarios can be evaluated to predict future CO_2 emissions from commercial aviation. It is with such applications in mind that the benefit of the *Fuel Estimation in Air Transportation (FEAT)* model order reduction framework becomes evident.

Disclaimers

This document has been created with elements of Base of Aircraft Data (BADA) Family 3 Release 3.15 which has been made available by EUROCONTROL to ETH Zurich (the Swiss Federal Institute of Technology Zurich). EUROCONTROL has all relevant rights to BADA.

EUROCONTROL shall not be liable for any direct, indirect, incidental or consequential damages arising out of or in connection with this document, including with respect to the use of BADA. The fuel burn models provided in SI M shall not be used for comparing fuel efficiency and emission data between aircraft models and manufacturers. Recommended model applications are reported in Section 3.5.

Acknowledgments

We would like to thank Dr. Peter Wild (Swiss International Air Lines) very much for providing valuable knowledge for our model fine tuning and its validation. We highly appreciate his support throughout the last months. Furthermore, we thank all industry experts that reviewed our work (foremost Mr. Urs Glarner), the BADA team from EUROCONTROL for the fruitful exchange (foremost Mr. Vincent Mouillet), and Mr. Thomas Noack (Planespotters.net) for providing us free data on the current aircraft fleet.

We would like to thank the Audi AG for the financial support to this work. This research project is part of the Swiss Competence Center for Energy Research in Efficient Technologies and Systems for Mobility (SCCER mobility) of the Swiss Innovation Agency Innosuisse.

Supplementary material

Supplementary data associated with this article can be found, in the online version, at https://doi.org/10.1016/j.trd.2020.102528.

References

Ahearn, M., Boeker, E., Gorshkov, S., Hansen, A., Hwang, S., Koopmann, J., Malwitz, A., Noel, G., Reherman, C., Senzig, D., Solman, G.B., Tosa, Y., Wilson, A., Zubrow, A., Dipardo, J., Majeed, M., Bernal, J., Biederman, A., Dinges, E., Rickel, D., Yaworski, M., 2017. Aviation Environmental Design Tool (AEDT) Technical Manual, Version 2d (Report no: DOT-VNTSC-FAA-17-16). U.S. Department of Transportation, Federal Aviation Administration. URL https://aedt.faa.gov/.

Airbus, 2019. Global Market Forecast: Cities, Airports & Aircraft 2019–2038, http://gmf.airbus.com/.

AirNav Systems, 2019. Aircraft ADS-B flight track data of January and August, 2018, purchased from AirNav Systems, RadarBox. https://www.radarbox24.com/flight-data.

ATAG, 2020. Fact Sheet: Tracking Aviation Efficiency. https://www.atag.org/our-publications/latest-publications.html.

Boeing, 2019. Commercial Market Outlook 2019–2038 of The Boeing Company. URL https://www.boeing.com/commercial/market/commercial-market-outlook/.

Coker, A., 2019. JetBlue rejoins cargo sector with more capacity for success (Article, 29.08.2019). https://www.freightwaves.com/news/jetblue-rejoins-cargo-sector-with-more-capacity-for-success.

Dalmau, R., Prats, X., Ramonjoan, A., Soley, S., 2020. Estimating fuel consumption from radar tracks: a validation exercise using FDR and radar tracks from descent trajectories. CEAS Aeronaut. J. 11, 355–365. https://doi.org/10.1007/s13272-020-00441-2.

Dray, L., 2013. An analysis of the impact of aircraft lifecycles on aviation emissions mitigation policies. J. Air Transp. Manage. 28, 62–69. https://doi.org/10.1016/j.jairtraman.2012.12.012. https://www.sciencedirect.com/science/article/pii/S0969699712001652?via%3Dihub.

Dray, L.M., 2018. Aviation Integrated Model 2015: Documentation. Air Transportation Systems Lab, UCL Energy Institute. http://www.atslab.org/aim-2015-documentation-v9-270120/.

EASA, 2019. ICAO Aircraft Engine Emissions Databank. European Union Aviation Safety Agency. https://www.easa.europa.eu/easa-and-you/environment/icao-aircraft-engine-emissions-databank.

EcoPower, 2020. Why Wash An Engine? EcoServices, LLC. http://www.ecopowerenginewash.com/WhyWash.php.

Eurostat, 2019. Eurostat transport database: Air transport measurement – passengers (avia_pa). Statistical Office of the European Union. https://ec.europa.eu/eurostat/web/transport/data/database.

FAA, 2017. Aviation Environmental Design Tool Version 2b - Uncertainty Quantification Report. U.S. Department of Transportation, Federal Aviation Administration. URL https://aedt.faa.gov/.

FOCA, 2019. Piston Aircraft Engine Emissions. Swiss Federal Office for Civil Aviation (FOCA). URL https://www.bazl.admin.ch/bazl/en/home/specialists/regulations-and-guidelines/environment/pollutant-emissions/aircraft-engine-emissions/report-appendices-database-and-data-sheets.html.

Glarner, U., 2019. Engine degradation and overhaul cycles: First-order approximation for medium- and long-haul aircraft. Private correspondence with Mr. Urs Glarner, Sr. Field Representative at the Customer Service of Pratt & Whitney/IAE International Aero Engines.

Graver, B., Zhang, K., Rutherford, D., 2019. CO2 emissions from commercial aviation, 2018 (Working paper 2019-16). International Council on Clean Transportation (ICCT). URL https://theicct.org/publications/co2-emissions-commercial-aviation-2018.

Hadjaz, A., Marceau, G., Savéant, P., Schoenauer, M., 2012. Online Learning for Ground Trajectory Prediction. In: SESAR 2nd Innovation Days, Nov 2012, Braunschweig, Germany. hal-00766049. Braunschweig, Germany. https://hal.inria.fr/hal-00766049.

IATA, 2019. Economic Performance of the Airline Industry, 2019 End-year report. International Air Transport Association. URL https://www.iata.org/contentassets/36695cd211574052b3820044111b56de/airline-industry-economic-performance-dec19-report.pdf.

ICAO, 2009. Traffic - Commercial Air Carriers Reporting Instructions, Form A. International Civil Aviation Organization. URL http://www.icao.int/staforms.

ICAO, 2017. ICAO Carbon Emissions Calculator Methodology. International Civil Aviation Organization. URL https://www.icao.int/environmental-protection/Carbonoffset/Pages/default.aspx.

ICAO, 2018. ICAO Long-Term Traffic Forecasts Passenger and Cargo. International Civil Aviation Organization. URL https://www.icao.int/sustainability/Documents/.

ICAO, 2019. 2019 Environmental Report: Aviation and Environment - Destination Green, The Next Chapter. International Civil Aviation Organization. URL https://www.icao.int/environmental-protection/Documents/.

IPCC, 1999. IPCC Special Report on Aviation and the Global Atmosphere Foreword Preface Summary. Intergovernmental Panel on Climate Change. URL https://www.ipcc.ch/pdf/special-reports/spm/av-en.pdf.

Kim, B., Fleming, G., Balasubramanian, S., Malwitz, A., Lee, J., Ruggiero, J., Waitz, I., Klima, K., Stouffer, V., Long, D., Kostiuk, P., Locke, M., Holsclaw, C., Morales, A., Mcqueen, E., Gillette, W., 2005. System for assessing Aviation's Global Emissions Technical Manual. Federal Aviation Administration. URL https://www.faa.gov/.

Kim, B.Y., Fleming, G.G., Lee, J.J., Waitz, I.A., Clarke, J.-P., Balasubramanian, S., Malwitz, A., Klima, K., Locke, M., Holsclaw, C.A., Maurice, L.Q., Gupta, M.L., 2007. System for assessing Aviation's Global Emissions (SAGE), Part 1: Model description and inventory results. Transp. Res. Part D: Transp. Environ. 12, 325–346. https://doi.org/10.1016/j.trd.2007.03.007. https://www.sciencedirect.com/science/article/pii/S1361920907000387.

Lee, J.J., Lukachko, S.P., Waitz, I.A., Schafer, A., 2001. Historical and future trends in aircraft performance, cost, and emissions. Annu. Rev. Energy Env. 26, 167–200. https://doi.org/10.1146/annurev.energy.26.1.167. http://web.mit.edu/aeroastro/sites/waitz/publications/Ann.Rev.reprint.pdf.

Lissys Ltd, 2008. Piano-X Aircraft Emissions and Performance User's Guide. Technical Report. URL www.piano.aero.

MIT, 2020. Traffic and Capacity by Operating Region. MIT Global Airline Industry Program, Airline Data Project. http://web.mit.edu/.

Mouillet, V., 2019. User Manual for the Base of Aircraft Data (BADA) Revision 3.15. Technical Report EUROCONTROL. URL https://www.eurocontrol.int/publication/user-manual-base-aircraft-data-bada.

Nuic, A., Poles, D., Mouillet, V., 2010. BADA: An advanced aircraft performance model for present and future ATM systems. Int. J. Adapt. Control Signal Process. 24, 850–866. https://doi.org/10.1002/acs.1176. http://doi.wiley.com/10.1002/acs.1176.

OAG Aviation Worldwide Limited, 2019. Historical schedules data for 2012 and 2018. https://www.oag.com/airline-schedules-data.

Oaks, R., Ryan, H., Paglione, M., 2010. Prototype implementation and concept validation of a 4-D trajectory fuel burn model application. In: AIAA Guidance, Navigation, and Control Conference. American Institute of Aeronautics and Astronautics, Reston, Virigina. https://doi.org/10.2514/6.2010-8164.

Olsen, S.C., Wuebbles, D.J., Owen, B., 2013. Comparison of global 3-D aviation emissions datasets. Atmos. Chem. Phys. 13, 429–441. https://doi.org/10.5194/acp-13-429-2013. URL www.atmos-chem-phys.net/13/429/2013/.

Pagoni, I., Psaraki-Kalouptsidi, V., 2017. Calculation of aircraft fuel consumption and CO2 emissions based on path profile estimation by clustering and registration. Transp. Res. Part D: Transp. Environ. 54, 172–190. https://doi.org/10.1016/j.trd.2017.05.006. https://www.sciencedirect.com/science/article/pii/S1361920916305533?via%3Dihub.

Planespotters, 2019. Global aircraft fleet data as of 2019–07-23. Data provided by Planespotters.net. https://www.planespotters.net/.

Poles, D., 2009. Base of Aircraft Data Aircraft (BADA) Aircraft Performance Modelling Report. EUROCONTROL Experimental Centre, European Organisation for the Safety of Air Navigation. URL www.eurocontrol.int.

Prats, X., Dalmau, R., Barrado, C., 2019. Identifying the Sources of Flight Inefficiency from Historical Aircraft Trajectories: A set of distance-and fuel-based performance indicators for post-operational analysis. In Thirteenth USA/Europe Air Traffic Management Research and Development Seminar (ATM2019). Vienna, Austria. URL http://www.atmseminarus.org/13th-seminar/.

Ryerson, M.S., Hansen, M., Bonn, J., 2014. Time to burn: Flight delay, terminal efficiency, and fuel consumption in the National Airspace System. Transp. Res. Part A: Policy Pract. 69, 286–298. https://doi.org/10.1016/j.tra.2014.08.024. https://linkinghub.elsevier.com/retrieve/pii/S0965856414002043.

Shell Aviation, 2014. Avgas 100LL Material Safety Data Sheet according to OSHA Hazard Communication Standard, 29 CFR 1910.1200. http://www.epc.shell.com/documentRetrieve.asp?documentId=131577295.

Sheng, H., Marais, K., Landry, S., 2015. Assessment of stratospheric fuel burn by civil commercial aviation. Transp. Res. Part D: Transp. Environ. 34, 1–15. https://doi.org/10.1016/j.trd.2014.10.008. https://www.sciencedirect.com/science/article/pii/S1361920914001497.

Simone, N.W., Stettler, M.E., Barrett, S.R., 2013. Rapid estimation of global civil aviation emissions with uncertainty quantification. Transp. Res. Part D: Transp. Environ. 25, 33–41. https://doi.org/10.1016/j.trd.2013.07.001.

Skowron, A., Lee, D., De León, R., 2013. The assessment of the impact of aviation NOx on ozone and other radiative forcing responses – The importance of representing cruise altitudes accurately. Atmos. Environ. 74, 159–168. https://doi.org/10.1016/j.atmosenv.2013.03.034. https://www.sciencedirect.com/science/article/pii/S1352231013002100?via%3Dihub.

USDOT, 2018. Air Carrier Statistics Form 41 Traffic: T-100 Segment (All Carriers). U.S. Department of Transportation, Bureau of Transportation Statistics. URL https://www.transtats.bts.gov/DataIndex.asp.

USDOT, 2019. Air Carrier Statistics Form 41 Financial Data: Schedule P-12(a). U.S. Department of Transportation, Bureau of Transportation Statistics. URL https://www.transtats.bts.gov/DataIndex.asp.

Wasiuk, D., Lowenberg, M., Shallcross, D., 2015. An aircraft performance model implementation for the estimation of global and regional commercial aviation fuel burn and emissions. Transp. Res. Part D: Transp. Environ. 35, 142–159. https://doi.org/10.1016/j.trd.2014.11.022. https://www.sciencedirect.com/science/article/pii/S1361920914001850#s0010.

Whiteley, M., 2018. European Aviation Fuel Burn and Emissions Inventory System for the European Environment Agency (for data from 2005, Version 2018.01) volume 01. EUROCONTROL, Pan-European Single Sky Directorate, Environment and Climate Change Section. https://www.eurocontrol.int/publication/european-aviation-fuel-burn-and-emissions-inventory-system-feis-european-environment.

Wild, P., 2019. Multiple expert interviews on aircraft operation and performance during 2019. Private correspondence with Dr. Peter Wild, Pilot (CMD) and Examiner/Instructor on A320/A220 at Swiss Airlines, President Transport Commission for Education, Research and Innovation at AeroSuisse, Managing Partner at Carbon Care.

Wilkerson, J.T., Jacobson, M.Z., Malwitz, A., Balasubramanian, S., Wayson, R., Fleming, G., Naiman, A.D., Lele, S.K., 2010. Analysis of emission data from global commercial aviation: 2004 and 2006. Atmos. Chem. Phys. 10, 6391–6408. https://doi.org/10.5194/acp-10-6391-2010. URL www.atmos-chem-phys.net/10/6391/2010/.

Winther, M., Rypdal, K., 2019. EMEP/EEA air pollutant emission inventory guidebook 2019. European Environment Agency (EEA). URL https://www.eea.europa.eu/publications/emep-eea-guidebook-2019.

Yanto, J., Liem, R., 2018. Aircraft fuel burn performance study: A data-enhanced modeling approach. Transp. Res. Part D: Transp. Environ. 65, 574–595. https://doi.org/10.1016/j.trd.2018.09.014. https://www.sciencedirect.com/science/article/pii/S1361920917309288.

Glossary

ADS-B: Automatic Dependent Surveillance-Broadcast
AEDT: Aviation Environmental Design Tool
AEM: Advanced Emission Model
APU: Auxiliary Power Unit
ATM: Air Traffic Management
BADA: Base of Aircraft Data
CORSIA: Carbon Offsetting and Reduction Scheme for International Aviation
EED: Engine Emissions Databank
FAA: Federal Aviation Administration
FEAT: Fuel Estimation in Air Transportation
FOCA: Swiss Federal Office for Civil Aviation
IATA: International Air Transport Association
ICAO: International Civil Aviation Organization
ICCT: International Council on Clean Transportation
IPCC: Intergovernmental Panel on Climate Change
ISA: International Standard Atmosphere
MTOW: Maximum Take-Off Weight
OAG: Official Airline Guide
ROCD: Rate Of Climb or Descent
RPK: Revenue Passenger-Kilometer
TEM: Total Energy Model
TOW: Take-Off Weight
VCAS: Calibrated Air Speed
VTAS: True Air Speed